The Simulation Model of the Vertical Dynamics and Control of an Elevator System

Xabier Arrasate[1], José M. Abete[2] and Stefan Kaczmarczyk[3]

[1] Fundamental Sciences, Mondragon Unibertsitatea, 20500 Arrasate-Mondragón, Euskadi, Spain, e-mail: jarrasate@eps.mondragon.edu

[2] Mechanical Engineering, Mondragon Unibertsitatea, 20500 Arrasate-Mondragón, Euskadi, Spain, e-mail; jmabete@eps.mondragon.edu

[3] Division of Engineering, School of applied Sciences, University of Northampton St. George's Avenue, Northampton NN2 6JD, UK, e-mail: stefan.kaczmarczyk@northampton.ac.uk

Keywords: elevator system, longitudinal vibration, drive machine dynamics, non-stationary distributed model, computer simulation

Abstract. A non-stationary distributed model of the vibration of an elevator system that accommodates the following aspects has been developed: machine and drive dynamics, the longitudinal response of the rope-car-counterweight system, the coupling effects across the traction sheave and the response to excitation sources such as the torque ripple. Hamilton's principle is applied to derive a set of partial differential equations that describes the dynamic behaviour of the mechanical part. These equations are discretized by expanding the longitudinal displacements in terms of the modal shapes to obtain a set of ordinary differential equations. The discrete model is then solved numerically in MATLAB-Simulink. Parameters of actual lift installations are used in the simulations to analyse the response of the system. Experimental tests are carried out in order to identify the system characteristics and to validate the simulation model.

Introduction

A lift installation can be represented as a system comprising two rigid masses representing the car and the counterweight suspended on hoist ropes, and the drive machine. One of the main problems in lift installations is to achieve and maintain adequate ride quality standards. Car ride quality can be compromised by excessive vibrations. Thus, an in-depth knowledge of its dynamic response and vibration characteristics are important to satisfy the ever-increasing ride performance requirements. The drive machine couples the car-rope and the counterweight-rope subsystems; it supplies energy into the system and often becomes a source of excitation. Therefore, the issue of influence of the drive machine dynamics on the overall performance of the lift system is of primary importance.
Ropes in elevator systems are usually represented as axially moving continua with lumped elements (car and counterweight) at their ends. Various elevator system models, lumped ones or distributed ones, stationary ones (where the rope length does not vary) or non-stationary ones (where the rope moves axially), have been developed and reported to study different aspects of their dynamics [1]. In the non-stationary case, the axial motion of the ropes is usually defined via the velocity profile determined by the application of an ideal drive machine model. Nevertheless, there are some studies where it is treated differently. For example, Fung et al. [2] analysed the coupling effects between the machine and the rope-car dynamics in a particular lift configuration where there was no counterweight and the rotor diameter varied as the rope was coiled onto a drum.
The work undertaken in this study addresses the development of a dynamic model of a lift system that accommodates the following main aspects: the machine and drive dynamics, the longitudinal response of the rope-car-counterweight system, the coupling effects across the traction sheave and the response to excitation sources such as a torque ripple.

Elevator System Model

Longitudinal Vibration Model. Details on the development of this part can be found in [3]. Figure 1 shows a 2:1 roping configuration of an elevator system and its schematic representation. The hoist rope of mass m per unit length, Young's modulus E and effective cross-sectional area A passes over the traction sheave. The mass of the car is m_c; the mass of the counterweight, m_w; the radius of the traction sheave is R; the length from the counterweight up to the sheave, $l(t)$; the total length of the rope, L; and I the moment of inertia of the sheave.

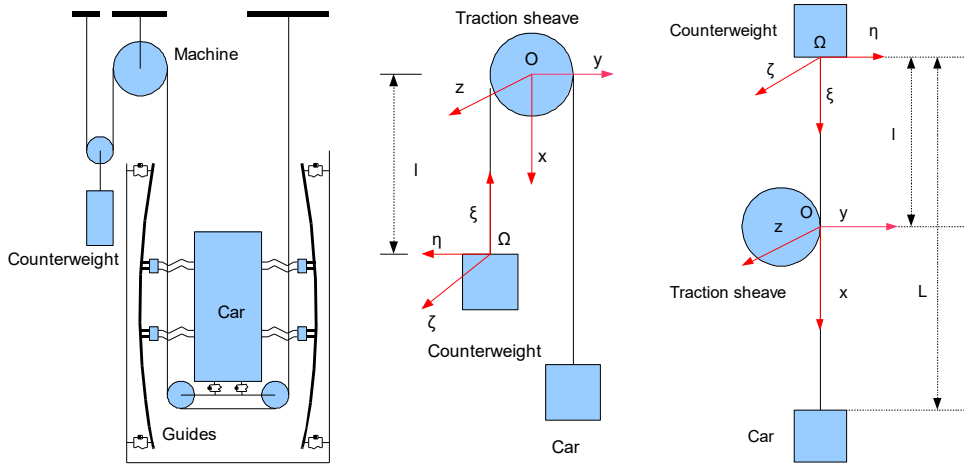

Fig.1: Schematic of a lift system and frames of reference

It has been assumed that the cable material is uniform, the sheave is perfectly rigid and that there is no rope slip across the sheave and only longitudinal motion is admitted in the car-rope and counterweight-rope subsystems. Two frames of reference are used: a coordinate system $\Omega\xi\eta\zeta$ attached to and moving with the counterweight treated as a perfectly rigid, and a stationary inertial system $Oxyz$ [4]. The undeformed position of any cable section measured from the counterweight frame is given by the spatial variable s.
Hamilton's principle is applied in order to obtain a set of partial differential equations as follows,

$$\begin{aligned} \rho_w(s)u_{w,tt} - EA\,u_{w,ss} &= \rho_w\left(\ddot{l} - g\right) \\ \rho_c(s)\,u_{c,tt} - EA\,u_{c,ss} &= \rho_c\left(\ddot{l} + g\right) \\ m_S\ddot{l} - EA\left[u_{w,s}(l,t) - u_{c,s}(l,t)\right] &= \frac{\tau}{R} \end{aligned} \tag{1}$$

where $u_w(s,t)$ and $u_c(s,t)$ are the rope dynamic displacements at the counterweight- and car-sides respectively , t is time, $()_s$ and $()_t$ denote partial differentiation with respect to s and t, respectively, $l(t)$ is the length of the rope at the counterweight side (the overdot denotes the total derivative with respect to time), g is the acceleration of gravity, $m_S=I/R^2$, $\tau(t)$ is the machine torque, $\rho_w(s)=m+\delta(s)m_w$, $\rho_c(s)=m+\delta(s-L)m_c$ and $\delta(s)$ is Dirac's delta function.
These equations are discretized by expanding the longitudinal displacements in terms of the modal shapes to obtain a set of non-linear ordinary differential equations with time-varying coefficients.

Drive System Model. The machine shaft speed is controlled in order for the car to follow a specific velocity profile to achieve good ride quality. A vector controller oriented to the magnets flux has been modelled and implemented in the simulation. The control system is composed of one velocity and two torque PI controllers. The drive system comprises a permanent magnet synchronous motor powered via an inverter that supplies a pulse width modulated (PWM) voltage [5,6].

Computer Simulations and Experimental Results

Elevator System Parameters. The values of the lift parameters chosen to carry out numerical simulations correspond to an actual installation. The suspension system comprises 6 standard wire ropes with m = 0.16 kg/m, $E = 1.43 \cdot 10^{11}$ N/m^2 and $A = 3.28 \cdot 10^{-5}$ m^2. Other parameters are m_c = 1450 kg, m_w = 1250 kg, R = 0.08 m and $I = 0.045$ kg·m^2. The length of the whole rope is L = 23 m.

Torque Ripple Frequencies. The permanent magnet synchronous motor has p = 16 poles, n = 48 slots and the slip is null. According to the literature [7], its theoretical frequencies can be calculated by the following expression

$$f_i = 2 f_s \left(\frac{n}{p} \pm i \right), \quad i = -1,0,1 \tag{2}$$

where f_s is a fundamental electrical frequency and equals $p/2$ times the shaft rotation frequency. Thus, taking into account that the rated speed is 1 m/s and the lift roping is 2:1, the fundamental frequency is 31.8 Hz.

In order to identify those excitation frequencies some measurements have been carried out [8] in the elevator system of Fig. 1. Accelerometers have been positioned on the machine, on the floor of the car and on each guide shoe, and spectra have been recorded during either upwards or downwards travel. The left graph on Fig. 2 shows the autospectrum measured by the accelerometer positioned on the floor of the car in the vertical direction during an upwards travel of the lift. The vibration magnitude is large up to 260 Hz, although a peak at 762 Hz is also worth considering. Therefore, attention has been paid to ripple frequencies below that one. According to Eq. 2, those frequencies are 127, 191 and 255 Hz during the constant velocity interval. The right graph on Fig. 2 shows the autospectrum measured by the accelerometer positioned on the machine in the vertical direction during the same travel, together with the same autospectrum on the left but up to 260 Hz. The torque ripple frequencies are clearly present, particularly the fundamental one. Some other peaks corresponding to the car modes appear on the spectrum. Besides, the frequency at 762 Hz previously mentioned is a harmonic of the one at 127 Hz (6 times it, actually). Those peaks are also present in the autospectra measured by the accelerometers positioned on the guide shoes.

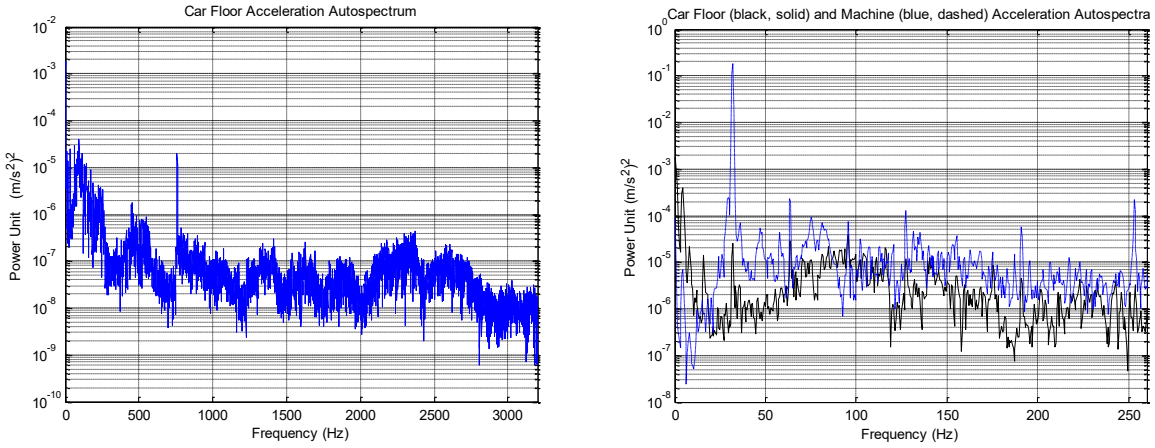

Fig. 2: Car floor and machine acceleration autospectra

Computer Simulations. Fig. 3 shows a simple schematic of the model, where the ripple has been taken as an oscillatory perturbation to be added to the machine torque. The perturbation is composed of four sinusoidal waves corresponding to the four frequencies shown in Fig. 2, where the amplitude of the first one will be 0.5 Nm and the one of the others 20 times smaller, according to the measured values of the machine acceleration.

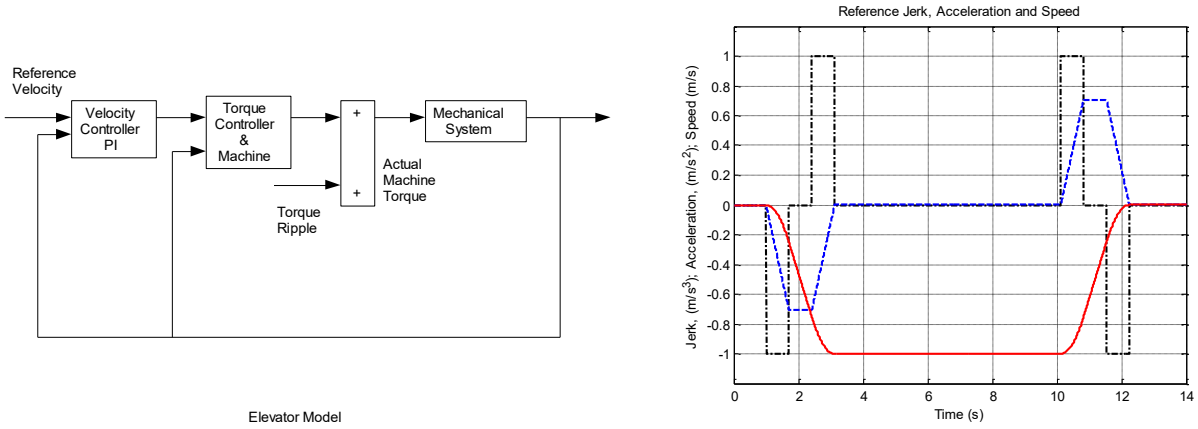

Fig. 3: Schematic of the elevator model and reference jerk (black, dash-dot), acceleration (blue, dashed) and speed (red, solid)

The elevator will carry out an upwards travel where the initial length of the counterweight side segment is 2 m. Initial displacement and velocity of any point of the rope are zero. Fig. 3 shows the reference jerk, acceleration and speed profiles to be followed by the car with the car acceleration and speed profiles obtained from the simulation being superimposed. Fig. 4 displays the actual car and counterweight accelerations obtained from the simulation.

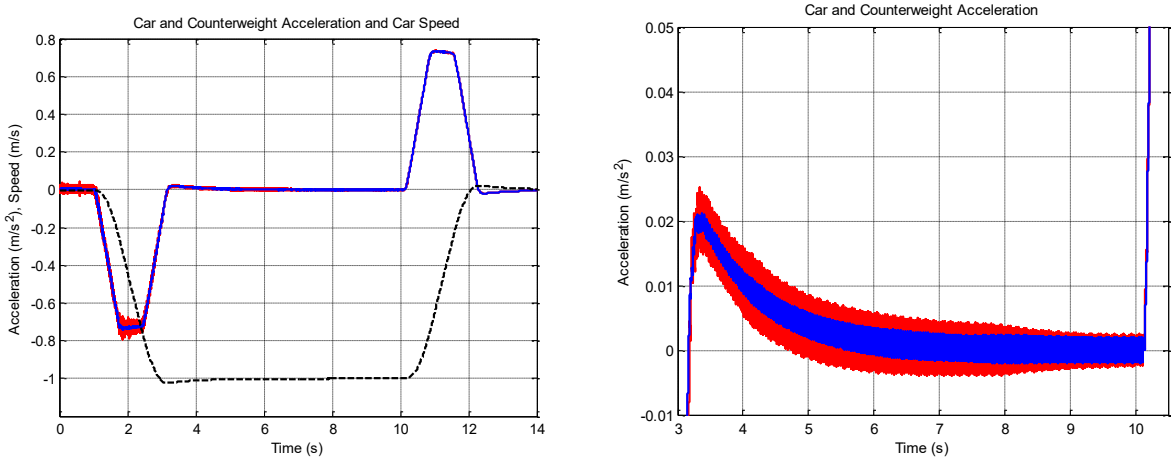

Fig. 4: Actual car acceleration (blue, solid), counterweight acceleration (red, solid) and car speed (black, dashed)

Convergence of the response has been achieved with a low number of modes [3]. The first five natural frequencies of the car- and counterweight-side ropes have been considered for the simulations. Fig. 5 shows their calculated evolution in time. The car-side rope frequencies increase during an upwards travel; counterweight-side ones decrease. According to Fig. 5, the first natural frequency of the counterweight is closer to the excitation frequency of 31.8 Hz at the beginning of the travel. Thus, it is evident from the plots presented in Fig. 4 that the magnitude of the counterweight-side rope vibration is higher than that of the car-side. Coupling through the traction sheave transmits vibration to the car-side.

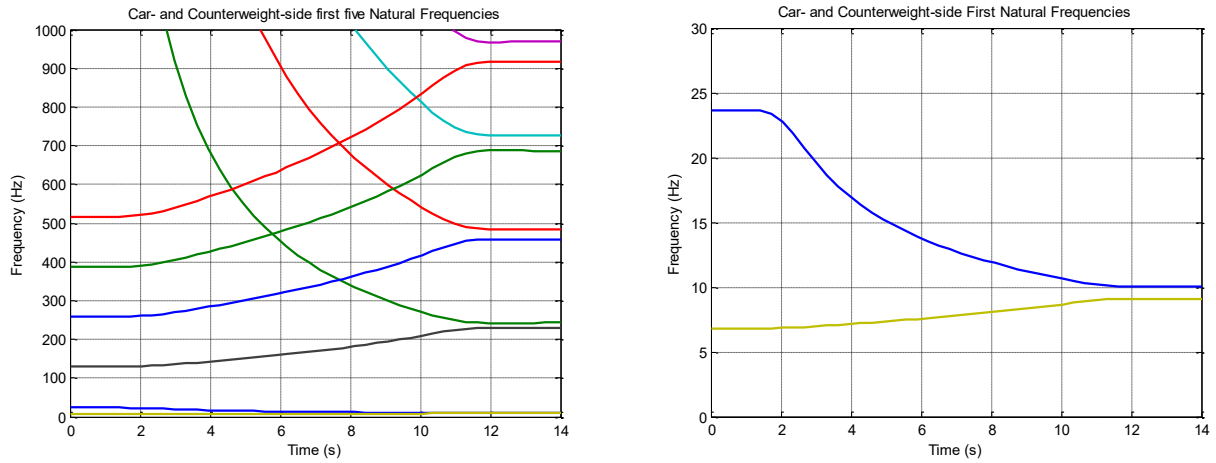

Fig. 5: Evolution of the first five natural frequencies with respect to time

Conclusions

The simulation predicts that when the frequency of the excitation caused by the machine torque is near the natural frequency range of the system, resonance phenomena take place. In addition, it is evident from the simulation results that adverse vibrational behaviour affecting car ride quality arise due to non-uniform acceleration/deceleration profiles and the coupling effects between the dynamics of the car and counterweight. It is expected that suitable compensation strategies can be applied in order to mitigate the effects of torque ripple and to control the response during the passage through resonance and caused by poor lift velocity/ acceleration profile.

Acknowledgment

This research has been sponsored by the Vertical Transport Group of MONDRAGON.

References

[1] X. Arrasate, J.M. Abete and S. Kaczmarczyk: The analysis and optimization of the dynamic behaviour and control of a lift system to achieve improved car ride quality. PhD Proposal, Mondragon Unibertsitatea, 2007
[2] R. Fung, J. Lin and C. Yao: Vibration analysis and suppression control of an elevator string actuated by a pm synchronous servo motor. Journal of Sound and Vibration, 206, 399 – 423, 1997.
[3] X. Arrasate, J.M. Abete and S. Kaczmarczyk: Distributed longitudinal vibration model of a lift system including the machine dynamics. 2nd IC-EpsMso, July 2007.
[4] S. Kaczmarczyk, J. Andrew and J. Adams: The modelling and prediction of the influence of building vibration on the dynamic response of elevator ropes. Materials Science Forum, 440-441, pp 489 – 496, 2003
[5] G. Almandoz, J. Poza, M.A. Rodríguez, A. González: Co-simulation tools for the permanent magnet machine design oriented to the application. EUROCON, pp 1687-1693, September 2007
[6] I. Boldea, S.A. Nasar: Electric Drives, CRC Press, 1999. ISBN 0-8493-2521-8
[7] M.P. Norton, D. G. Karczub: Fundamentals of noise and vibration analysis for engineers, Cambridge University Press, 2003, ISBN 0521499135
[8] Bruel & Kjaer Technical Project Description, Project 13050: Feasibility Study on Application of SPC Techniques for Elevator Cabins.